Mutagenesis Study of the 2Fe-2S Center and the FAD Binding Site of the Na^+-Translocating NADH:Ubiquinone Oxidoreductase from *Vibrio cholerae*[†]

Blanca Barquera,*[,‡] Mark J. Nilges,[§] Joel E. Morgan,[‡] Leticia Ramirez-Silva,[‡,||] Weidong Zhou,[‡] and Robert B. Gennis[‡]

Department of Biochemistry, University of Illinois at Urbana-Champaign, 600 South Mathews Avenue, Urbana, Illinois 61801, and The Illinois EPR Research Center, 506 South Mathews Avenue, Urbana, Illinois 61801

Received June 23, 2004; Revised Manuscript Received July 9, 2004

ABSTRACT: Many marine and pathogenic bacteria have a unique sodium-translocating NADH:ubiquinone oxidoreductase (Na^+-NQR), which generates an electrochemical Na^+ gradient during aerobic respiration. Na^+-NQR consists of six subunits (NqrA-F) and contains five known redox cofactors: two covalently bound FMNs, one noncovalently bound FAD, one riboflavin, and one 2Fe-2S center. A stable neutral flavin-semiquinone radical is observed in the air-oxidized enzyme, while the NADH- or dithionite-reduced enzyme exhibits a stable anionic flavin-semiquinone radical. The NqrF subunit has been implicated in binding of both the 2Fe-2S cluster and the FAD. Four conserved cysteines (C70, C76, C79, and C111) in NqrF match the canonical 2Fe-2S motif, and three conserved residues (R210, Y212, S246) have been predicted to be part of a flavin binding domain. In this work, these two motifs have been altered by site-directed mutagenesis of individual residues and are confirmed to be essential for binding, respectively, the 2Fe-2S cluster and FAD. EPR spectra of the FAD-deficient mutants in the oxidized and reduced forms exhibit neutral and anionic flavo-semiquinone radical signals, respectively, demonstrating that the FAD in NqrF is not the source of either radical signal. In both the FAD and 2Fe-2S center mutants the line widths of the neutral and anionic flavo-semiquinone EPR signals are unchanged from the wild-type enzyme, indicating that neither of these centers is nearby or coupled to the radicals. Measurements of steady-state turnover using NADH, Q-1, and the artificial electron acceptor ferricyanide strongly support an electron transport pathway model in which the noncovalently bound FAD in the NqrF subunit is the initial electron acceptor and electrons then flow to the 2Fe-2S center.

The sodium-translocating NADH-ubiquinone oxidoreductase (Na^+-NQR) was first found in the marine bacterium *Vibrio alginolyticus* (*1*, *2*). The enzyme oxidizes NADH and reduces ubiquinone (*3*). Driven by this redox reaction, Na^+-NQR also functions as an energy-conserving primary sodium pump, transporting Na^+ ions electrogenically from the cytoplasm to the periplasmic space. The Na^+ gradient generated in this way is used as an energy source for such cellular processes as flagellar rotation and amino acid transport (*4*, *5*). Interestingly, as more bacterial genomes have been sequenced, Na^+-NQR has been found in bacteria that are not marine species, among them a number of pathogens including *Haemophilus influenzae*, *Vibrio cholerae*, *Yersinia pestis*, and *Neisseria meningitides* (*6*−*8*).

Studies of the enzyme from *Vibrio alginolyticus*, *Vibrio harveyi*, and *Vibrio cholerae* have shown that Na^+-NQR is a ca. 210 kDa complex composed of six subunits (designated as NqrA-F), and that the genes coding for the six subunits reside together in one operon (*7*−*11*).The NqrA, C, and F subunits are relatively hydrophilic while the NqrB, D, and E subunits are hydrophobic. The enzyme contains a noncovalently bound FAD, a noncovalently bound riboflavin, two covalently bound FMNs, and an iron−sulfur center as cofactors (*7*, *12*, *13*). The two FMNs are covalently linked to threonine residues in the NqrB and NqrC subunits (*8*, *14*, *15*).

The original Na^+-NQR gene sequence was initially obtained from *V. alginolyticus* almost concurrently by two different groups (*9*, *10*). In studying these data, Rich et al. (*16*) identified three motifs in the sequence of the NqrF subunit which they proposed to be (1) the site for NADH substrate binding, (2) the binding site for an FAD cofactor, and (3) the site of an iron−sulfur center. Today, with a growing number of bacterial genomes published, Na^+-NQR sequences from a number of bacteria are available. Alignment of these sequences (*17*) shows clearly that the three motifs identified by Rich et al. (*16*) are conserved across all Na^+-NQRs (Figure 1).

The FAD binding motif was identified on the basis of homology to toluate 1,2-dioxygenase and benzoate 1,2-dioxygenase (*16*). The FAD motif can be seen in the results of a BLAST search (*18*) for sequences with homology to NqrF (Figure 2). The idea that NqrF contains a noncovalently

[†] This research was supported by NIH Grant HL16011 (R.B.G.).

* Author to whom correspondence should be sent. Current address: Department of Biology, Center for Biotechnology & Interdisciplinary Studies, 1W14 Jonsson-Rowland Science Center, Rensselaer Polytechnic Institute, 110 Eighth St., Troy, NY 12180-3590. Tel: (518) 276-6446. E-mail: barqub@rpi.edu.

[‡] University of Illinois at Urbana-Champaign.

[§] The Illinois EPR Research Center.

[||] On sabbatical from Departamento de Bioquímica, Facultad de Medicina, Apdo. Postal 70-159, Universidad Nacional Autonóma de México, 04510, México, D.F., Mexico.

10.1021/bi048689y CCC: $27.50
Published on Web 08/31/2004

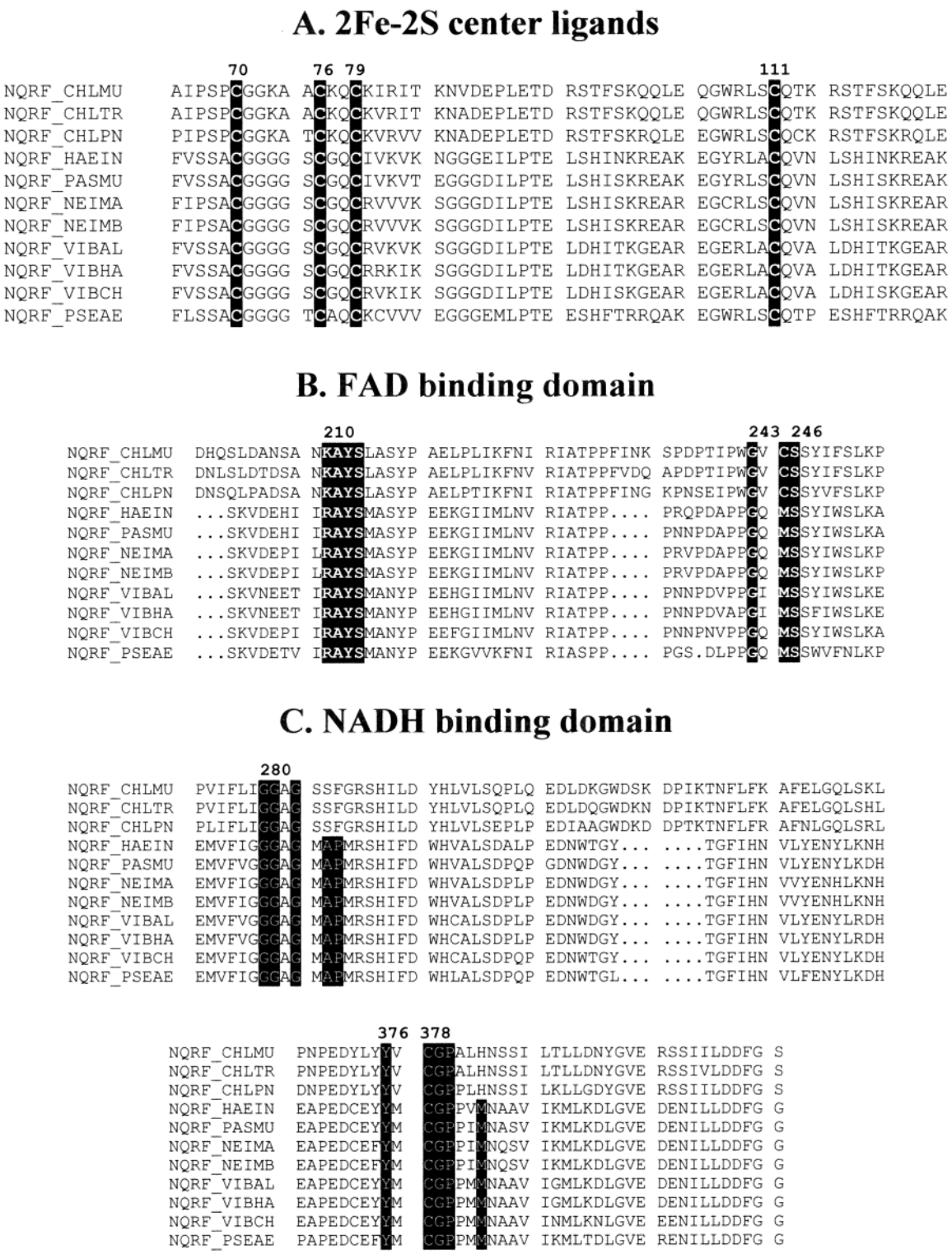

FIGURE 1: Partial alignment of the NqrF sequence from several bacteria showing the conserved motifs which include the candidate residues for (A) iron−sulfur center ligands (C70, C76, C79, and C111) (B) FAD binding site (R210, Y212, S246), and (C) NADH binding site. Key to sequences: NQRF_CHLMU, *Chlamydia muridarum*, Swiss bank accession number **Q9PLI3**; NQRF_CHLTR, *Chlamydia trachomatis*, Swiss bank accession number **O84745**; NQRF_CHLPN, *Chlamydia pneumoniae*, Swiss bank accession number **Q9Z723**; NQRF_HAEIN, *H. influenzae*, Swiss bank accession number **O05012**; NQRF_PASMU, *Pasteurella multocida*, Swiss bank accession number **Q9CLA6**; NQRF_NEIMA, *N. meningitides* (serogroup A), Swiss bank accession number **Q9JVQ3**; NQRF_NEIMB, *N. meningitides* (serogroup B), Swiss bank accession number **Q9K0M8**; NQRF_VIBAL, *V. alginolyticus*, Swiss bank accession number **Q56584**; NQRF_VIBHA, *V. harveyi*, Swiss bank accession number **Q9RFV6**; NQRF_VIBCH, *V. cholerae*, Swiss bank accession number **Q9X4Q8**; NQRF_PSEAE, *Pseudomonas aeruginosa*, Swiss bank accession number **Q9HZL1**.

bound FAD cofactor is also supported by biochemical evidence; FAD has been found in an isolated protein fraction which consisted mainly of NqrF (*12*).

Additional structural information about this flavin-binding motif comes from Nishida et al. (*19*). In a structural comparison of several other flavin-dependent enzymes, three

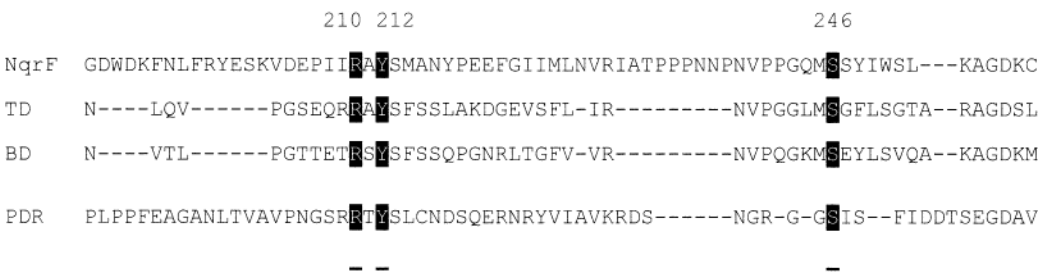

FIGURE 2: Sequence alignment for several flavoproteins. **NqrF** is the NqrF subunit of Na^+-NQR from *V. cholerae*; **TD** is toluate 1,2-dioxygenase from *P. aeruginosa*; **BD** is benzoate 1,2-dioxygenase from *Acinetobacter calcoaceticus*; **PDR** is phthalate dioxygenase reductase from *Burkholderia cepacia*; **FNR** is ferredoxin-NADP reductase from *Buchnera aphidicola*; **NR** is nitrate reductase beta chain NarH from *Staphylococcus aureus*; **b5R** is NADH-cytochrome b5 reductase from human. Highlighted residues are conserved across Na^+-NQR and the other flavoproteins listed.

conserved amino acids (Arg, Tyr, and Ser/Thr) were identified to be of particular importance for flavin binding. These amino acids reside in a β-barrel domain and form hydrogen bonds to the flavin. This is the same motif identified by Rich et al. (*16*) in the NqrF subunit. In *V. cholerae*, the three key residues correspond to R210, Y212, and S246. These residues are fully conserved across all Na^+-NQR sequences found to date.

The iron−sulfur motif is marked by four conserved cysteines: C70, C76, C79, and C111 (*V. cholerae* numbering). This motif was initially proposed to anchor a 4Fe-4S cluster, on the basis of homology between NqrF and several known 4Fe-4S-containing enzymes including ferredoxin (*16*). Subsequent electron paramagnetic resonance (EPR) spectroscopic studies on the purified enzyme from *V. alginolyticus* revealed a signal ($g_{xy} \cong 1.94$) which could be assigned to a 2Fe-2S center, but no signal consistent with a 4Fe-4S center was found (*13*, *20*). Recently, further questions have been raised about the origin of the EPR signal. It has been suggested that the signal is not from Na^+-NQR at all, but arises from an iron−sulfur center in a contaminant of the preparation (*21*).

The EPR spectrum of reduced Na^+-NQR also contains a signal now assigned to an anionic flavin radical (*22*). In the oxidized form of the enzyme (as isolated), a flavin radical is also present, but here the radical is a neutral flavin semiquinone. In both the reduced and oxidized enzyme preparations, the EPR signal corresponds to about 1 equiv/mol of enzyme (*22*). Recent studies have suggested that the neutral and anionic radicals arise from two different flavin components of the enzyme (*23*). The identification of which of the four flavins are responsible for these radicals and what the functional roles might be is essential to understanding how this redox-driven sodium pump works.

The Na^+-NQR operon from *V. cholerae* has recently been cloned into a plasmid and the recombinant protein expressed in *V. cholerae* (*24*) with a histidine tag on the C-terminus of NqrF. This has made it possible to use site-directed mutagenesis to investigate the assignments of the FAD and iron−sulfur sites made on the basis of the motifs described above. In the present work, the three conserved residues in the FAD binding motif have been mutated to alanine or leucine, and each of the four conserved cysteines in the iron−sulfur center motif have been mutated to alanine. The results clearly demonstrate that these residues are necessary for binding the FAD and 2Fe-2S cluster, as expected from the sequence motifs. Notably, mutation of any of the four conserved cysteines to alanine results in the complete loss of the 2Fe-2S EPR signal, demonstrating unequivocally that the 2Fe-2S EPR signal arises from an iron−sulfur center in the Na^+-NQR and is not from a contaminating protein. Additionally, the EPR spectroscopy demonstrates that the absence of either the FAD or 2Fe-2S cluster has no influence on either the amount or nature of the flavin semiquinone species.

MATERIALS AND METHODS

Strains and Growth. The O395N1-*toxT:lac::*Δ*nqrA-F* strain of *V. cholerae* was used as host for the expression of wild-type and mutant Na^+-NQR. Cells were grown in LB medium at 37 °C. *Escherichia coli* Top10 competent cells (Invitrogen) were used for mutagenesis.

Site Directed Mutagenesis. The plasmid pBAD-*nqr* was used both as the template for mutagenesis and as the expression vector of the recombinant Na^+-NQR from *V. cholerae* (*25*). For each mutation a pair of primers was designed. Additional restriction sites were built into the primers to facilitate identification of mutated plasmids by restriction enzyme digestion. The sequence of the forward primer from each pair is given in Table 1. Primers were synthesized by the University of Illinois Biotechnology Center. Mutagenesis was carried out using the "QuikChange" kit (Stratagene). Mutated plasmids were identified by restriction enzyme digestion and further confirmed by DNA sequencing. The resulting plasmids were then transformed into *V. cholerae* O395N1-*toxT:lac::*Δ*nqrA-F* by electroporation.

Enzyme Purification. Wild-type and mutant Na^+-NQR was purified using Ni-NTA as described previously (*8*). Purified enzyme was passed through a desalting column (D-Salt Polyacrylamide 6000, Pierce) using a buffer ("final buffer") containing 50 mM sodium phosphate, pH 8.0, 100 mM NaCl, 5% glycerol, 10 mM EDTA, and 0.05% DM, frozen in aliquots, and kept at liquid nitrogen temperature. Protein concentrations were determined using the BCA Protein Assay Kit from Pierce, and SDS−PAGE containing 6 M urea (4−16% acrylamide) was used to check the purity of the proteins.

Enzymatic Activity. Na^+-NQR transports electrons from NADH to the ubiquinone pool in the membrane. The physiological acceptor is believed to be ubiquinone-8 (Q-8) (*13*, *24*). When the activity of the purified enzyme is assayed in vitro, ubiquinone-1 (Q-1), a relatively hydrophilic analogue

Table 1: Primers Designed for 2Fe-2S Center and FAD Binding Site Mutagenesis

mutation	sequence of forward primer[a]
2Fe-2S center	
C70A-F	5′-GGTGTATTCGTATCTTCCGCG**GCT**GGTGGTGGTGGTTCATG
C76A-F	5′-GTGGTGGTGGTGGTTCC**GCG**GGCCAATGCCGTGTAAAAATC
C79A-F	5′-GGTGGTTCATGTGGCCAA**GCC**CGGGTAAAAATCAAATCAGG
C111A-F	5′- GAAGGTGAGCGTTTGGCT**GCG**CAGTGCTGTAAAAGCAG
FAD	
R210L-F	5′- CTAAAGTGGATGAGCCAATAATA**TTA**GCATACTCAATGGCG
Y212L-F	5′- GATGAGCCAATCATCCGAGCT**CTC**TCAATGGCGACCTACC
S246A-F	5′- GCCACCAGGCCAAATG**GCC**AGTTACATCTGGTCACTGAAAG

[a] Bold letters indicate the mutation.

of Q-8, can be used as electron acceptor. The activity of the enzyme can be assayed spectrophotometrically, by following either the oxidation of NADH (which has a maximum at 340 nm) or the reduction of Q-1 (which has a maximum at ca. 282 nm but which overlaps the NADH; see below). The purified enzyme is also able to transfer electrons from NADH to the artificial electron acceptor ferricyanide. This appears to be a short-circuit of the normal pathway of electron flow in the enzyme (*26*).

Assays of steady-state enzyme turnover were carried out using a full-spectrum method. The reaction is started by adding enzyme to a cuvette containing both the electron donor and acceptor substrates. In a total volume of 1.0 mL, the assay mixture typically contains 0.1 mM NADH, 0.1 mM Q-1 (or 1 mM potassium ferricyanide), 200 mM NaCl, and 20 mM Tris-HCl, pH 8.0. Spectra were acquired using an Agilent 8453 diode array spectrophotometer at intervals of 0.5 s. Data acquisition is commenced a few seconds before the reaction is started and is typically continued until one or both substrates are exhausted.

Analysis of the full-spectrum assay data was carried out as follows. The spectrum from the final time point was subtracted from every line in the raw data matrix (**A**), resulting in a data matrix that reflects only the absorbance changes (difference spectra data matrix = **D**). This was then analyzed in one of two ways, (1) basis set analysis or (2) analysis at selected wavelengths.

(1) In basis set analysis, a basis set (**B**) was constructed of reduced-minus-oxidized spectra of the individual substrates in the reaction (NADH and Q-1 or NADH and ferricyanide), normalized to a standard concentration, using published extinction coefficients: NADH at 340 nm, 0.0062 μM^{-1}; Q-1 at 248 − 268 nm, 0.0078 μM^{-1}; ferricyanide at 420 nm 0.001 μM^{-1}. This two-spectrum basis set was augmented with a trivial spectrum: a vector consisting of ones at every wavelength. Each time-point spectrum in the difference spectra data matrix was then decomposed with respect to the basis set, using the MLDIVIDE ("\") function of MATLAB (The Mathworks, Natick, MA). This produced a set of time-course vectors (**V**) corresponding to the components in the basis set which give the concentration of the component at each time point. In order to check the quality of this fit, a theoretical difference spectra matrix was constructed from the basis set and the time-course vectors (**T** = **C′***__V__), and a matrix of residuals obtained by subtracting this theoretical matrix from the difference spectra data matrix (**R** = **D** − **T**).

(2) The canonical method for the second type of analysis is to monitor the reaction at selected wavelengths or to monitor the absorption difference for wavelength pairs: NADH at 340 nm, ferricyanide at 420 nm, and quinol at 248 − 268 nm (*1*). These data could also be extracted from the difference spectra data matrix.

In either case the rate of the reaction could be determined from the initial slope from the time-course data.

EPR Spectroscopy. EPR measurements were performed on a Varian-122 X-band (9.08 GHz) spectrometer equipped with an Air Products Helitran cyrostat. A microwave power of 0.02 mW was used with a modulation amplitude of 2 G at 100 kHz. The magnetic field was calibrated with a Varian gaussmeter, and the microwave frequency was determined with an EIP frequency meter. Air-oxidized and anaerobically reduced samples (dithionite or NADH) in quartz tubes (3 mm inside diameter) were frozen in an *n*-pentane−dry ice slurry, and spectra were acquired at 40 K. Spin concentrations were determined by double integrating baseline corrected spectra. For calibration, a sample containing 1 mM $CuSO_4$ in a 20% glycerol solution was run at the same power and temperature used for the protein samples.

UV−Visible Spectroscopy. UV−visible spectra of air-oxidized enzyme in "final buffer" were recorded on a Shimadzu UV-2101 PC spectrophotometer.

Flavin Analysis by Denaturation and Visible Spectroscopy. Enzyme was first denatured by addition of 6 M guanidine hydrochloride. After denaturation of the protein, all flavins can be expected to be spectroscopically equivalent. The total amount of flavin in the sample was determined from its UV−visible spectrum. The sample was then passed through a Centricon filter (molecular mass cutoff 3 kDa) to remove the protein and with it the covalently bound flavins. The amount of flavin in the resulting filtrate was again determined by UV−visible spectroscopy.

HPLC Analysis of Noncovalently Bound Flavins. The filtrate obtained as described above was also analyzed by HPLC as described previously (*25*).

RESULTS

Design of Mutants. The conserved motifs in NqrF identified by Rich et al. (1995) (*16*) are shown in Figure 1. In the numbering of the *V. cholerae* sequence, the key conserved residues in the FAD motif are R210, Y212, and S246. The key residues in the 2Fe-2S center motif are the four conserved cysteines: C70, C76, C79, and C111. Site-directed mutagenesis was used to replace each of these residues, as described in Table 1. The three residues in the FAD motif were changed to amino acids with aliphatic side chains, which would not be able to form hydrogen bonds to a flavin,

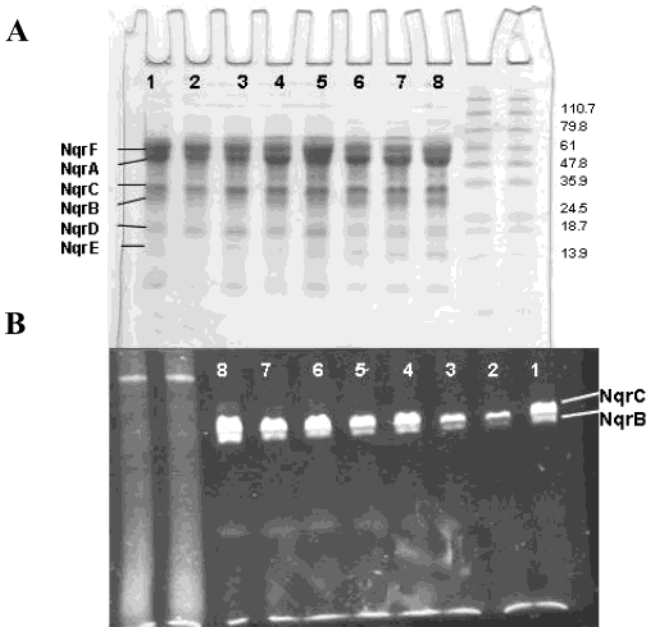

FIGURE 3: Urea−SDS−PAGE of the purified wild-type and mutant enzymes. (A) Coomassie stained gel. (B) Gel under UV illumination; the two fluorescent bands correspond to NqrB and NqrC, which contain covalently bound FMNs. Lane assignments: (1) C70A, (2) C76A, (3) C79A, (4) C111A, (5) R210L, (6) Y212L, (7) S246A, (8) wild-type.

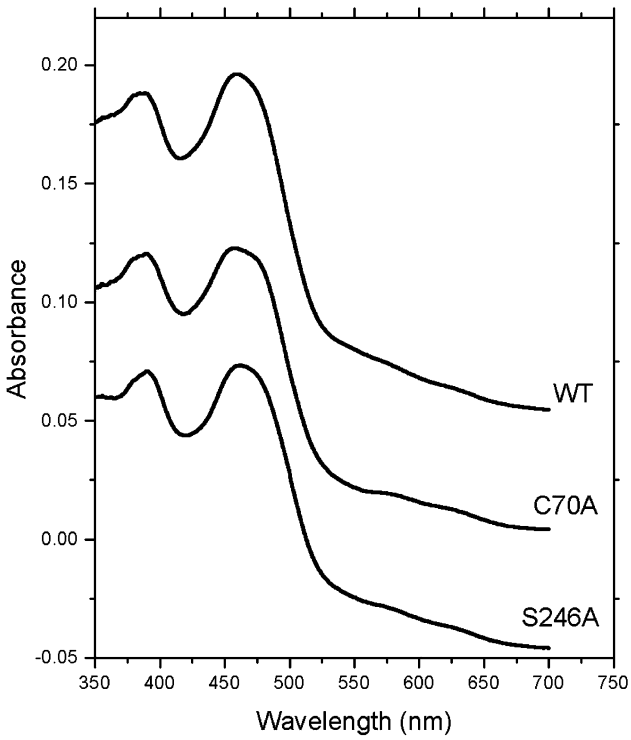

FIGURE 4: UV-visible absorbance spectra of air-oxidized Na^+-NQR: wild-type enzyme, C70A mutant, and S246A mutant. Approximately 3 μg of each protein, in "final buffer," was used for recording the spectra.

while each of the four cysteines in the iron−sulfur motif was converted to alanine.

Purification of Mutants. The four mutants within the iron−sulfur center motif and the three FAD binding motif mutants were purified by affinity chromatography on Ni-NTA. In each case, all six subunits can be identified on a urea polyacrylamide gel **(**Figure 3A). The NqrB and NqrC protein bands in the SDS−PAGE gel fluoresce under UV illumination, indicating that the two covalently bound FMNs are incorporated in all of the mutants (Figure 3B; this picture was obtained prior to staining). It is important to note that the level of expression, the yield from the purification, and the stability of the mutant proteins are not as high as for the wild-type.

UV−Visible Spectroscopy. Absorbance spectra of the wild-type and mutant enzymes were obtained from the air-oxidized (as isolated) form of the protein. All of the mutants exhibited the typical features of the Na^+-NQR complex, including the dominant peak at 450−460 nm, characteristic of flavins. Examples are shown in Figure 4.

Analysis of Flavin Content. The total amount of covalently and noncovalently bound flavin in each preparation was measured using the guanidine denaturation/ultrafiltration protocol described in Material and Methods. Results are presented in Table 2. For the wild-type enzyme, the results are consistent with the presence of four flavins, two in the low molecular weight fraction and two in the high molecular weight fraction. This is in agreement with our previous conclusion that there are two noncovalently bound flavins and two covalently bound flavins (*24*). The four 2Fe-2S center mutants (C70A, C76A, C79A, and C111A) all had essentially the same flavin content as the wild-type enzyme, with the same distribution between high and low molecular weight fractions. This indicates that, although the 2Fe-2S center resides in the same subunit as the FAD (NqrF), disruption of the iron−sulfur center does not alter the binding of the FAD.

Table 2: Flavin Content in Wild-Type and Mutants of Na^+-NQR

strain	flavin content[a]	filtrate/total[b]
WT	3.91 ± 0.143	0.54
2Fe-2S center mutants		
NqrF-C70A	3.695 ± 0.146	0.466
NqrF-C76A	3.9351 ± 0.366	0.499
NqrF-C79A	3.74 ± 0.145	0.504
NqrF-C111A	3.8 ± 0.238	0.51
FAD mutants		
NqrF-R210L	2.9 ± 0.115	0.38
NqrF-Y212L	2.8 ± 0.147	0.298
NqrF-S246A	3.05 ± 0.1799	0.32

[a] Millimoles of flavin after guanidine denaturation/millimoles of protein. An extinction coefficient of 12 mM^{-1} cm^{-1} was used. The standard deviation is given using four different samples. [b] Total amount of flavin after 6 M guanidine treatment. "Filtrate" represents the supernatant fraction after filtration of the guanidine denatured protein. A filter with molecular mass cutoff of 3 kDa was used.

In the case of the FAD binding site mutants, the substitution of any one of the three key amino acids in the FAD binding motif eliminates the presence of one flavin from the supernatant. In the three mutants analyzed (R210L, Y212L, and S246A) the total content of flavin in the protein is approximately three: two in the high molecular weight fraction and one in the low molecular weight fraction. The presence of the two covalently bound flavins is consistent with the presence of the two fluorescent bands in SDS gels (Figure 3B).

Analysis of Noncovalently Bound Flavin. The flavin content of the low molecular weight fraction (above) was analyzed by HPLC as described in Materials and Methods. This method was used previously (*25*) to demonstrate that

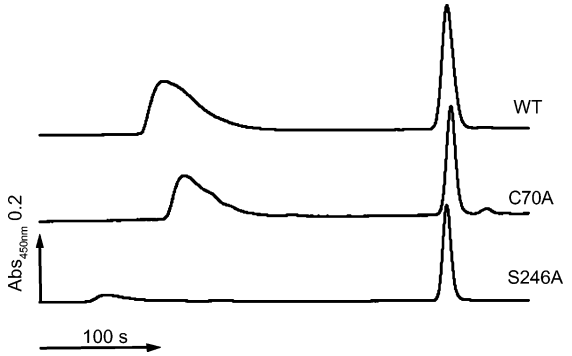

FIGURE 5: HPLC elution profile of the soluble flavins from denatured Na^+-NQR: wild-type and mutants. Ten nanomoles of each enzyme was denatured using 6 M guanidine and filtered using a Centricon ultrafiltration device (3 kDa molecular mass cutoff) and the filtrate injected into the HPLC.

Na^+-NQR contains 1 equiv of riboflavin in addition to the noncovalently bound FAD. As shown in Figure 5, the amount of FAD in the C70A mutant is essentially the same as in the wild-type, whereas, in the S246A mutant, there is only a small residual amount of FAD. All the enzyme preparations contain riboflavin.

Electron Paramagnetic Resonance Spectroscopy. When reduced by NADH or dithionite, wild-type Na^+-NQR exhibits two EPR signals. One, with $g = 2.0034$, has been assigned as an anionic flavo-semiquinone radical (*22*, *24*). The other, with $g_x \sim g_y = 1.9343$, $g_z = 2.0182$, is typical of 2Fe-2S centers (*27*). The EPR signals in the oxidized and reduced wild-type enzyme were quantified by double integration and compared to a copper sulfate standard. (See Material and Methods.)

In order to quantitate the spin concentrations associated with the various EPR signals, a sample of wild-type Na^+-NQR with a protein concentration of 83 μM was divided between two EPR tubes. One sample was kept in the initial air-oxidized state while the other was reduced anaerobically by the addition of 10 mM NADH. The air-oxidized state, where the only signal is the neutral flavoquinone radical, gave a spin concentration of 70 μM (±10%). Thus, the neutral radical is present in between 75% and 92% of the enzyme molecules. This fraction is probably higher since there is a small amount of extraneous protein in the enzyme preparation.

In the reduced sample the spin concentration increased to 170 μM concomitant with the appearance of the 2Fe-2S signal. As the concentration of the flavin radical under NADH reduction is very close to the concentration of the flavin radical under oxidizing conditions (*24*), the spin concentration of the 2Fe-2S center is approximately equal to that of the Na^+-NQR protein (±10%). These results reinforce the conclusion that the 2Fe-2S is a bona fide component of the enzyme.

As shown in Figure 6A, the iron−sulfur EPR signal is completely absent from the spectra of all four cysteine mutants. This result unambiguously confirms the assignment of the 2Fe-2S EPR spectrum as arising from an intrinsic cofactor of Na^+-NQR.

In contrast, in the spectra of NADH reduced samples, all three mutants in the putative FAD binding site (R210L, Y212L and S246A) still exhibit the $g = 1.9343$ and 2.0182 features, showing that the 2Fe-2S center is present in all three mutants (Figure 6B). With S246A the amplitude of the 2Fe-2S signal is essentially the same as in the wild-type enzyme.

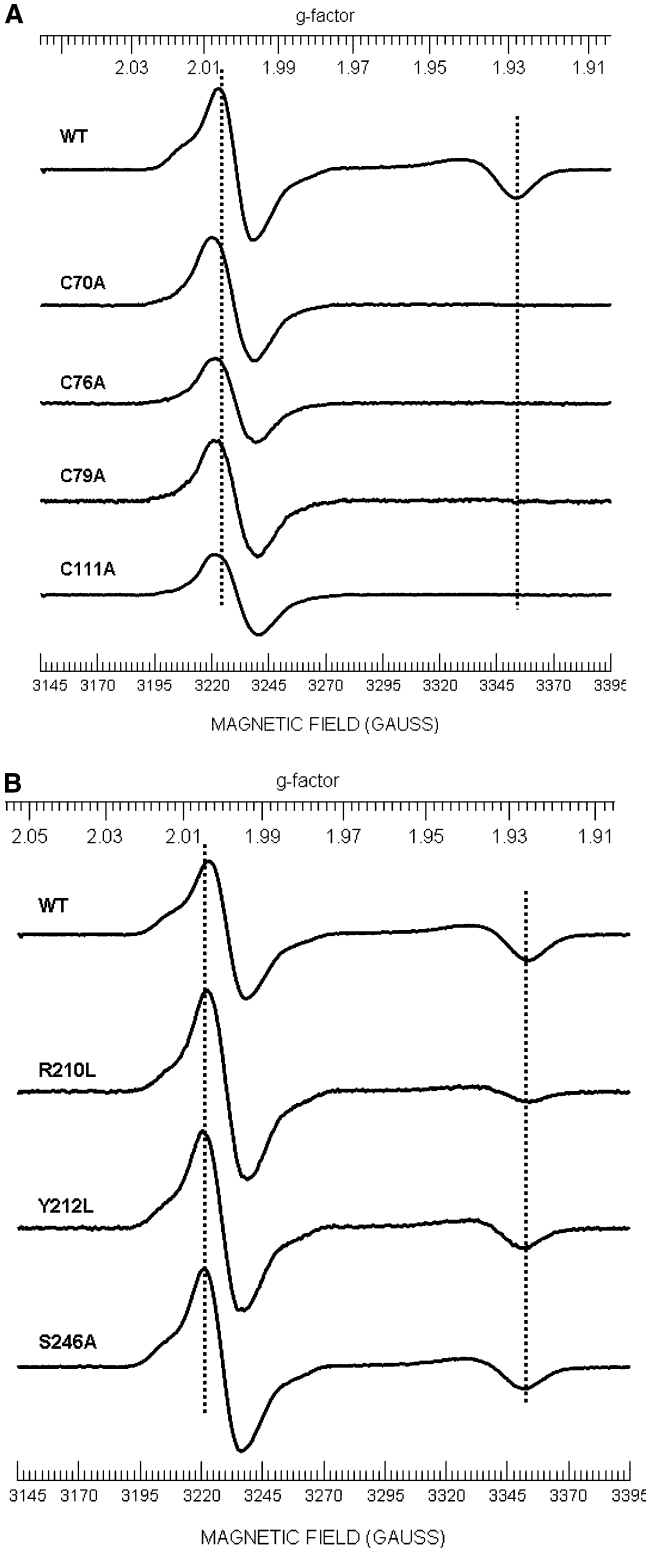

FIGURE 6: X-band EPR spectra of NADH anaerobically reduced Na^+-NQR: wild-type and mutants: (A**)** 2Fe-2S center motif mutants; (B) FAD binding motif mutants. Protein concentration was approximately 100 μg/mL in each case; 10 mM NADH was used in all cases. The dotted vertical line on the left indicates the position of the 2Fe-2S center signal ($g \sim 1.94$) while the dotted vertical line on the right indicates the position of the radical ($g \sim 2.003$). Note that the 2Fe-2S signal includes an additional feature which appears as a shoulder on the low-field side of the radical signal. The spectral conditions are reported in Materials and Methods.

Table 3: Properties of the Flavin Radicals in Wild-Type and Mutants of Na^+-NQR

strain	neutral flavin radical: air−oxidized (line width in Gauss)	anionic flavin radical: NADH reduced[a] (line width in Gauss)	anionic flavin radical: dithionite reduced[b] (line width in Gauss)
WT	19.9	15.2	14.4
2Fe-2S center mutants			
NqrF-C70A	20.1	18.5	14.9
NqrF−C76A	20.3	18.3	13.1
NqrF-C79A	20.4	17.8	13.3
NqrF-C111A	20.3	17.7	13.2
FAD mutants			
NqrF-R210L	20.7	16.6	13.6
NqrF-Y212L	20.7	15.3	13.4
NqrF-S246A	20.1	15.6	13.7

[a] 10 mM NADH as reductant. [b] 60 mM dithionite as reductant.

With Y212L the amplitude is slightly smaller. With R210L the signal is significantly diminished, but both *g*-value resonances are still clearly discernible. This is consistent with the fact that the R210L enzyme is less stable than the other preparations. In the dithionite reduced samples, the variation in the amplitudes of the 2Fe-2S center signal among the three FAD mutants is much smaller.

In contrast, neither of the two types of radical signals was abolished in any of the seven mutants, although small changes may have occurred. The neutral and anionic flavosemiquinone radical signals are distinguished by a clear difference in line width. In the case of the wild-type enzyme, the line widths (peak-to-trough of the first derivative) of the neutral radical in the air-oxidized enzyme and the anionic radical in the dithionite-reduced enzyme are 19.9 and 14.4 G, respectively. When NADH is used as reductant, the line width is 15.2 G, a result that would be consistent with the presence of subpopulations of both types of radicals (*22*). For each of the seven mutants, the line width of the flavin radical signal was measured in air-oxidized, NADH-reduced, and dithionite-reduced samples. The results are shown in Table 3. In the case of the air-oxidized and dithionite-reduced samples, in every case the line width was approximately the same as with the wild-type enzyme, around 20 and 14 G, respectively. In the case of the NADH-reduced samples, the measured line widths were all intermediate between these values, but clearly smaller, in each case, than for the oxidized enzyme.

Enzymatic Activity. The NADH:quinone oxidoreductase activity of wild-type and all mutant enzymes was measured, using a full-spectrum assay (see Materials and Methods) that could follow both oxidation of NADH (Figure 7A) and the reduction of either Q-1 (Figure 7B) or the artificial electron acceptor ferricyanide (Figure 7C). To avoid side reactions, the assays were carried out under low O_2 conditions. All four cysteine mutants behaved similarly, exhibiting very low NADH:Q-1 oxidoreduction activity (3%) compared to the wild-type. All of the FAD binding site mutants (R210L, Y212L, and S246A) also exhibited extremely low NADH:Q-1 activity (S246A had about 10% activity, consistent with the amount of residual FAD present). However, NADH:ferricyanide oxido-reductase activity exhibited a different pattern (Figure 7C). The three FAD binding site mutants exhibited very low activity, whereas the four 2Fe-2S center mutants were as active as the wild-type enzyme. These results suggest that FAD precedes the 2Fe-2S center in the order of electron transport within the enzyme (Figure 8).

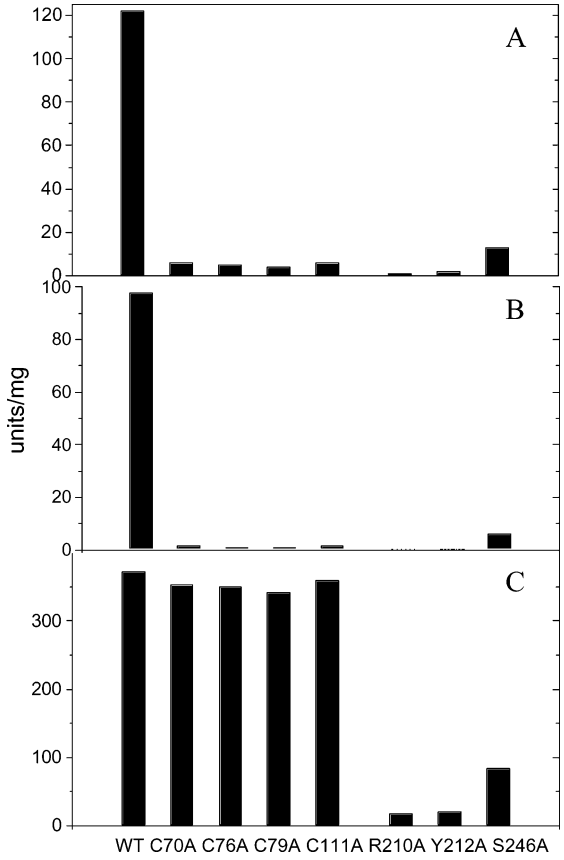

FIGURE 7: Steady-state turnover activity of wild-type and mutant Na^+-NQR: (A) NADH:Q-1 oxidoreduction measured by following NADH oxidation; (B) NADH:Q-1 oxidoreduction measured by following Q-1 reduction; (C) NADH:ferricyanide oxidoreduction measured by following reduction of ferricyanide. See Materials and Methods.

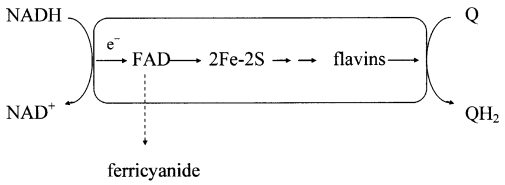

FIGURE 8: A scheme of the proposed electron transport pathway in Na^+-NQR. The noncovalently bound FAD in the NqrF subunit is the first cofactor to accept electrons from substrate NADH; the electrons then go to the 2Fe-2S center. The reduced FAD can be oxidized by ferricyanide directly.

DISCUSSION

The amino acid sequence of subunit F of Na^+-NQR contains motifs which have been predicted to be the binding sites for a 2Fe-2S center and a noncovalently bound FAD (*16*). Site-directed mutants have now been made in which each of the key amino acids which make up these motifs have been individually changed: C70A, C76A, C79A, and C111A for the predicted 2Fe-2S center, and R210L, Y212L, and S246A for the predicted FAD binding site (Figures 1 and 2).

All four cysteine-to-alanine mutations result in specific loss of the 2Fe-2S center. In all four mutants, the EPR signal

assigned to the 2Fe-2S center is absent, but it appears that all four flavin cofactors are still present. In all four mutants, subunits NqrB and NqrC in SDS−PAGE gels fluoresce under ultraviolet light (Figure 3B), indicating that, in each case, both of these subunits retain their covalently bound FMN moiety. The HPLC analysis of noncovalently bound flavins in C70A (Figure 5) indicates that both FAD and riboflavin are still present, and the UV−visible spectrum of this enzyme (Figure 4A) shows no large loss of flavin. The EPR spectra indicate that both the neutral (not shown) and anionic (Figure 6A) forms of the semiquinone radical are present. In the wild-type enzyme and all of the mutants, when dithionite is used as reductant, there is almost full occupancy of the anionic radical species (13−15 G). When NADH is used as reductant, the line width is larger, consistent with a mixture of anionic and neutral species. Under these conditions the EPR line width with each of the cysteine mutants is larger than with the wild-type enzyme (17−18.5 G compared to 15.2 G; see Table 3). This variation in line width may arise from small changes in the ratio of the populations of anionic and neutral flavin radicals. In order to understand these differences, it will probably be necessary to carry out a complete EPR-redox titration.

All three mutations in the putative FAD binding site result in the specific loss of all, or almost all, of the FAD in the enzyme, while the other flavins appear to be retained. In each case, the flavin analysis shows that approximately half of the noncovalently bound flavin is absent, and the HPLC analysis shows the specific loss of FAD from S246A mutant enzyme. The fluorescence observed in the SDS−PAGE gel (Figure 3B) shows that the covalently bound flavins in subunits NqrB and NqrC are retained in all three mutants while HPLC analysis of the flavin content of S246A shows that riboflavin is still present. EPR spectra indicate that each of the three mutants retains the 2Fe-2S center, and is able to exhibit both the anionic and neutral (not shown) (Figure 6B) forms of the semiquinone radical. This shows definitively that the FAD in the NqrF subunit is not the origin of either the anionic or the neutral radical signal.

Assays of steady state NADH:quinone oxidoreductase activity of the mutants show that loss of either the 2Fe-2S center of the FAD cofactor inactivates the enzyme. However, the mutations that eliminate the 2Fe-2S center have levels of NADH:ferricyanide oxidoreductase activity similar to that of the wild-type enzyme, whereas the mutants that eliminate the FAD lack the NADH:ferricyanide oxidoreductase activity (Figure 7). Hence, FAD must be the initial electron acceptor from NADH, and must be the site of interaction of ferricyanide. The electron flow must be NADH → FAD → 2Fe-2S center. The quinone reductase site must follow the 2Fe-2S center, whereas ferricyanide reductase activity requires only the FAD to be present.

In summary, the current work confirms that the FAD and the 2Fe-2S cofactors are bound by the predicted motifs in subunit F. It is now unambiguously clear that the 2Fe-2S EPR signal is not due to an impurity in the preparation (*21*), but arises from the enzyme itself, and can be assigned to the iron−sulfur center in subunit F. Within the NqrF subunit the order of electron flow is NADH → FAD → 2Fe-2S. Neither the neutral nor the anionic flavin-semiquinone is associated with the FAD component, and neither is influenced by the absence of the 2Fe-2S center. The continued application of site-directed mutagenesis should be helpful to identify which of the remaining three flavin components of Na^+-NQR are responsible for the observed radicals and what their functional roles might be in pumping Na^+ across the membrane.

ACKNOWLEDGMENT

We thank the staff of the Chemistry Machine Shop at the University of Illinois for their skillful help constructing the anaerobic cell.

REFERENCES

1. Unemoto, T., and Hayashi, M. (1993) Correlation between the respiration-driven Na^+ pump and Na^+-dependent amino acid transport in moderately halophilic bacteria, *J. Bioenerg. Biomembr. 25*, 385−391.
2. Dimroth, P. (1997) Primary sodium ion translocating enzymes, *Biochim. Biophys. Acta 1318*, 11−51.
3. Hayashi, M., Nakayama, Y., and Unemoto, T. (2001) Recent progress in the Na^+-translocating NADH-quinone reductase from the marine *Vibrio alginolyticus*, *Biochim. Biophys. Acta 1505*, 37−44.
4. Dibrov, P. A., Kostyrko, V. A., Lazarova, R. L., Skulachev, V. P., and Smirnova, I. A. (1986) The sodium cycle. I. Na^+-dependent motility and modes of membrane energization in the marine alkalotolerant *Vibrio alginolyticus*, *Biochim. Biophys. Acta 850*, 449−457.
5. Dibrov, P. A., Lazarova, R. L., Skulachev, V. P., and Verkhovskaya, M. L. (1986) The sodium cycle. II. Na^+-coupled oxidative phosphorylation in *Vibrio alginolyticus* cells, *Biochim. Biophys. Acta 850*, 458−465.
6. Hayashi, M., Nakayama, Y., and Unemoto, T. (1996) Existence of Na^+-translocating NADH-quinone reductase in *Haemophilus influenzae*, *FEBS Lett. 381*, 174−176.
7. Zhou, W., Bertsova, Y. V., Feng, B., Tsatsos, P., Verkhovskaya, M. L., Gennis, R. B., Bogachev, A. V., and Barquera, B. (1999) Sequencing and preliminary characterization of the Na^+-translocating NADH:ubiquinone oxidoreductase from *Vibrio harveyi*, *Biochemistry 38*, 16246−16252.
8. Barquera, B., Häse, C. C., and Gennis, R. B. (2001) Expression and mutagenesis of the NqrC subunit of the NQR respiratory Na^+ pump from *Vibrio cholerae* with covalently attached FMN, *FEBS Lett. 492*, 45−49.
9. Beattie, P., Tan, K., Bourne, R. M., Leach, D., Rich., R. P., and Ward, F. B. (1994) Cloning and sequencing of four structural genes for the Na^+-translocating NADH-ubiquinone oxidoreductase of *Vibrio alginolyticus*, *FEBS Lett. 356*, 333−338.
10. Hayashi, M., Hirai, K., and Unemoto, T. (1994) Cloning of the Na^+-translocating NADH-quinone reductase gene from the marine bacterium *Vibrio alginolyticus* and the expression of the beta-subunit in *Escherichia coli*, *FEBS Lett. 356*, 330−332.
11. Nakayama, Y., Hayashi, M., and Unemoto, T. (1998) Identification of six subunits constituting Na^+-translocating NADH-quinone reductase from the marine *Vibrio alginolyticus*, *FEBS Lett. 422*, 240−242.
12. Hayashi, M., and Unemoto, T. (1986) FAD and FMN flavoproteins participate in the sodium-transport respiratory chain NADH: quinone reductase of a marine bacterium, *FEBS Lett. 202*, 327−329.
13. Pfenninger-Li, X. D., Albracht, S. P. J., van Belzen, R., and Dimroth, P. (1996) NADH:ubiquinone oxidoreductase of *Vibrio alginolyticus*: purification, properties, and reconstitution of the Na^+ pump, *Biochemistry 35*, 6233−6242.
14. Nakayama, Y., Yasui, M., Sugahara, K., Hayashi, M., and Unemoto, T. (2000) Covalently bound flavin in the NqrB and NqrC subunits of Na^+-translocating NADH-quinone reductase from *Vibrio alginolyticus*, *FEBS Lett. 23723*, 1−4.
15. Hayashi, M., Nakayama, Y., Yasui, M., Maeda, M., Furuishi, K., and Unemoto, T. (2000) FMN is covalently attached to a threonine residue in the NqrB and NqrC subunits of Na^+-translocating NADH-quinone reductase from *Vibrio alginolyticus*, *FEBS Lett. 24493*, 1−4.

16. Rich, P. R., Meunier, B., and Ward, F. B. (1995) Predicted structure and possible ion motive mechanism of the sodium-linked NADH-ubiquinone oxidoreductase of *Vibrio alginolyticus*, *FEBS Lett. 375*, 5−10.
17. Corpet, F. (1988) Multiple sequence alignment with hierarchical clustering, *Nucleic Acids Res. 16*, 10881−10890.
18. Smith, R. F., Wiese, B. A., Wojzynski, M. K., Davison, D. B., and Worley, K. C. (1996) BCM search launcher- an integrated interface to molecular biology data base search and analysis services available on the World Wide Web, *Genome Res. 6*, 454−462.
19. Nishida, H., Inaka, K., and Miki, K. (1995) Specific arrangement of three amino acid residues for flavin-binding barrel structures in NADH-cytochrome b5 reductase and the other flavin-dependent reductases, *FEBS Lett. 361*, 97−100.
20. Bogachev, A. V., Murtazina, R. A., and Skulachev, V. P. (1997) The Na^+/e^- stoichiometry of the Na^+-motive NADH: Quinone oxidoreductase in *Vibrio alginolyticus*, *FEBS Lett. 409*, 475−477.
21. Steuber J, R. M., Fritz G, Neese F, Dimroth P. (2002) Inactivation of the Na^+-translocating NADH:ubiquinone oxidoreductase from *Vibrio alginolyticus* by reactive oxygen species, *Eur. J. Biochem. 269*, 1287−1292.
22. Barquera, B., Morgan, J. E., Lukoyanov, D., Scholes, C. P., Gennis, R. B., and Nilges, M. J. (2003) X- and W-band EPR and Q-band ENDOR studies of the flavin radical in the Na^+-translocating NADH:quinone oxidoreductase from *Vibrio cholerae, J. Am. Chem. Soc. 125*, 265−275.
23. Bogachev AV, B. Y., Ruuge, E. K, Wikström, M., Verkhovsky, M. I. (2002) Kinetics of the spectral changes during reduction of the Na^+-motive NADH:quinone oxidoreductase from *Vibrio harveyi*, *Biochim. Biophys. Acta 1556*, 113−120.
24. Barquera, B., Hellwig, P., Zhou, W., Morgan, J. E., Häse, C. C., Gosink, K., Nilges, M., Bruesehoff, P. J., Roth, A., Lancaster, C. R.D., and Gennis, R. B. (2002) Purification and characterization of the recombinant Na^+-translocating NADH:quinone oxidoreductase from *Vibrio cholerae*, *Biochemistry 41*, 3781−3789.
25. Barquera, B., Zhou, W., Morgan, J. E., and Gennis, R. B. (2002) Riboflavin is a component of the Na^+-pumping NADH:quinone oxidoreductase from *Vibrio cholerae*, *Proc. Natl. Acad. Sci. U.S.A. 99*, 10322−10324.
26. Tokuda, H., and Unemoto, T. (1984) Na^+ is translocated at NADH: quinone oxidoreductase segment in the respiratory chain of *Vibrio alginolyticus*, *J. Biol. Chem. 259*, 7785−7790.
27. Aliverti, A., Hagen, W. R., and Zanetti, G. (1995) Direct electrochemistry and EPR spectroscopy of spinach ferredoxin mutants with modified electron transfer properties, *FEBS Lett. 368*, 220−224.

BI048689Y